Malaysian Journal of Chemistry, 2023, Vol. 25(5), 13-22
(Special Issue: *4th International Symposium on Multidisciplinary Science 2022*)

Facile Preparation and Characterisation of Oxygen-rich Reduced Graphene Oxide for Improved Electrochemical Performance: A Preliminary Study

Mohamad Aliff Bin Ali Rahman[1], Soon Poh Lee[3,4], Kwok Feng Chong[3,4] and Ellie Yi Lih Teo[1,2*]
[1]Institute of Ecosystem Science Borneo, Universiti Putra Malaysia, 97008 Bintulu, Sarawak, Malaysia
[2]Department of Science & Technology, Faculty of Humanities, Management & Science, Universiti Putra Malaysia, 97008 Bintulu, Sarawak, Malaysia
[3]Faculty of Industrial Sciences & Technology, Universiti Malaysia Pahang Al-Sultan Abdullah, 26300 Gambang, Kuantan, Pahang Darul Makmur, Malaysia
[4]Centre for Advanced Intelligent Materials, Universiti Malaysia Pahang Al-Sultan Abdullah, 26300, Kuantan, Pahang Darul Makmur, Malaysia
*Corresponding author (e-mail: ellie_teo@upm.edu.my)

Graphene is an excellent candidate as an electrode material for supercapacitors due to its exceptional properties. Among the many synthesis routes, reduced graphene oxide (rGO) synthesised through modified Hummers' method followed by reduction has been the preferred route to obtain graphene due to its flexibility. Depending on the reaction condition, the degree of oxidation present on rGO will differ and affect its overall charge storage capability. But, the use of toxic reagents or harsh conditions will introduce environmental concerns. Herein, an environmental-friendly KCl was introduced to modify the degree of oxidation on rGO using a simple aggregation method. In this study, graphite oxide obtained through modified Hummers' method was modifiedwith KCl followed by reduction using ammonia to produce chemically-modified rGO (S-rGO).S-rGO obtained was then characterised using UV-Vis and FT-IR while its electrochemical behaviourwas studied with cyclic voltammetry. The UV-Vis and FT-IR analyses showed that the oxidationlevel of S-rGO increased linearly with the mass of KCl used. Specific capacitance calculated from the CV curves revealed that a 3.5 times enhancement was observed. The results revealed the possible modification on S-rGO using environmental-friendly KCl and its potential use as an electrode material for supercapacitors application.

Keywords: Surface modification; reduced graphene oxide; oxygen; aggregation; electrode

Received: June 2022; Accepted: December 2022

Historically, the theory of nanotechnology was first conceived by Richard Feynman in the 1960s [1], which Norio Taniguchi later defined in 1974, the term nanotechnology as "…the processing of separation, consolidation, and deformation of materials by one atom or one molecule" [2]. In 2004, the successful extraction of 2-dimensional graphene layers via repeating micromechanical exfoliation revitalised and sparked a golden age of research and development for advanced nanomaterial with promising breakthroughs in various fields and applications [3], [4].

Graphene is a unique carbon allotrope with outstanding properties such as high electrical conductivity and optical transparency [5], attributed to its one-atom-thick layer and sp^2-hybridised hexagonal lattice arrangement. Research on graphene as an electrode material in electrical energy storage systems has been lively over the past two decades. However, the commercial implementation of graphene-based technology is almost non-existent due to several limitations such as; 1) impractical top-down synthesis pathways e.g., micromechanical exfoliation can only produce small amounts of graphene as well as, 2) expensive and complex bottom-up synthesis pathways via chemical vapour deposition (CVD) still hinder the upscale production of graphene [6].

Reduced graphene oxide (rGO) is a cost-effective substitute that shares similar physical, chemical and electrical traits with graphene. This material can be easily synthesised through the oxidation of bulk graphite material, forming GO precursor which can be reduced to minimise the presence of surface oxygen groups (hence the term reduced GO) [7]. Alternatively, recent findings on the use of rGO with varying degrees of oxidation as an active material for electrodes in electrical energy storage systems such as supercapacitors [8], redox flow batteries [9], [10], and lithium-ion batteries [11], showed improvements towards their electrochemical and capacitance performances.

---

†Paper presented at the 4th International Symposium on Multidisciplinary Science 2022 (SMS 2022)

Various techniques have been introduced to tune the amounts of oxygen functionalities on rGO. Previously, Chen et al. successfully synthesised partially reduced GO via microwave irradiation [8]. The material, rich with surface oxygen groups, exhibited a hybrid behaviour of pseudo-capacitance (due to faradaic redox reaction) and electric double-layer capacitance which improved its overall electrochemical performance. Chemical reduction is another cost-effective parameter to control the degree of oxidation on rGO. Morimotoet al. studied the effect of different ratios between hydrazine and GO during reduction and concluded that synthesised rGO with an oxygen content of 20-40wt% was the most practical for energy storage, catalyst support and biosensor applications [12]. Similarly, chemical modification has been commonly utilised to preserve surface oxygen groups or introduce heteroatoms such as nitrogen or phosphorus on rGO to improve its electrochemical performances [13], [14]. Additionally, Cao et al. studied the effect of oxygen functionalities on the capacitance performance of thermally-reduced graphene oxide [15]. Further oxidation of GO was done via acid treatment prior to the thermal reduction. The authors recorded a decreasing trend in the capacitance performance of the electrode as the reduction temperature increased which supports the positive role of oxygen groups in improving capacitance on rGO. However, these treatments required the use of harmful and toxic reagents such as acid/basic and harsh conditions (e.g., high temperature) to manipulate the surface heteroatom functionalities which may raise air and water pollution concerns during the upscaling production of rGO.

An environmental-friendly technique was first proposed by Chen et al. who introduced KCl salt during the chemical reduction of GO [16]. The authors found that the KCl-assisted rGO had improved dispersion stability in an aqueous medium which contributed to its improved capacitance. However, no study has investigated the effect of KCl concentration on the degree of oxidation of rGO. In the present study, rGO with varying degrees of oxidation was successfully synthesised by adding different amounts of KCl salt during the chemical modification step. This preliminary study confirmed the successful reduction of GO using ammonia and the presence of oxygen functional groups on chemically modified rGO using UV-Vis absorbance and FT-IR analyses. The electrochemical performance of the as-synthesised rGO was also analysed using cyclic voltammetry (CV) analysis.

EXPERIMENTAL

1. Chemicals and Materials

All chemicals and reagents were commercially purchased from Merck, Sigma-Aldrich, R&M Chemicals, HmbG Chemicals and Bendosen. The materials were directly used without additional purification.

2. Preparation of Chemically Modified Reduced Graphene Oxide

2.1. Synthesis of Graphite Oxide

Graphite oxide was synthesised using the modified Hummers' method [17], which involved two reaction steps; pre-treatment and oxidation of graphite precursor. The synthesised product will be abbreviated as GO.

Initially, graphite powder (4.00 g; size < 50 µm; 99.5%) was dissolved in concentrated H_2SO_4, followed by the addition of P_2O_5 (6.00 g) and $K_2S_2O_8$ (6.00 g). The mixture was refluxed at 80 °C for 6 hours and cooled before it was diluted in distilled water. The treated graphite was filtered under vacuum and thoroughly washed to neutral pH before it was left to dry under reduced pressure.

Next, the pre-treated graphite (2.00 g) was dissolved in concentrated H_2SO_4 and stirred in an ice bath until it homogenised. $KMnO_4$ (17.50 g) was then added slowly to the mixture. It was refluxed at 35 °C for 4 hours and cooled before the mixture was transferred into a clean beaker. Distilled water (450.0 mL) was added in small portions to the mixture with constant stirring to maintain a temperature of ~90 °C. H_2O_2 solution (50.0 mL; 30%) was added drop by drop to the suspension and left to cool overnight. The reaction mixture was filtered under vacuum, followed by several washing with 1:10 HCl solution, distilled water, ethanol and diethyl ether. The final product was left to dry under reduced pressure [18].

2.2. Chemical Modification of Graphite Oxide

The chemical modification of graphite oxide was modified based on Rajagopalan and Chung [14]. Graphene oxide suspension (2.00 mg mL^{-1}) was prepared by dissolving dried GO (0.20 g) in distilled water, followed by exfoliation in an ultrasonic bath for 25 minutes. KCl salt (3.00 g and 5.00 g) was dissolved and the mixture was stirred at ambient temperature for 16 hours. The graphene oxide aggregates were filtered under vacuum and rinsed with small amounts of distilled water and ethanol before it was dried under reduced pressure. The final products will be abbreviated as 3SGO and 5SGO respectively.

2.3. Synthesis of Reduced Graphene Oxide

The chemical reduction of graphite oxide was modified based on Pham et al. [19]. Graphene oxide suspension (1.00 mg mL^{-1}) was prepared using similar steps described in subsection 2.2 and the suspension was transferred into a round-bottomed flask. Ammonia solution was added to the flask and the reaction mixture was refluxed at 80 °C for 12 hours. The mixture was filtered under vacuum and rinsed with distilled water and ethanol. The solid product was oven-dried at 80 °C for 12 hours. Similar steps were also repeated for 3SGO and 5SGO. The reduced products will be abbreviated as rGO, 3S-rGO and 5S-rGO respectively.

3. Electrode Preparation

The glassy carbon electrode (GCE) was treated by sequential polishing with alumina powders of different sizes (1.0 µm, 0.3 µm and 0.05 µm) and rinsed with deionised water before it was dried under reduced pressure. The electrode ink was prepared by dissolving rGO samples (2.0 mg/mL) in ethanol, followed by sonication for 1 hour to form a homogeneous mixture. The ink (20 µL) was drop-casted onto the pre-polished GCE and dried under reduced pressure before analysis.

4. Characterisation Methods

4.1. UV-Vis Spectrophotometer

All samples were prepared into 125 ppm suspensions using similar steps described in subsection 2.2. The suspensions were analysed using Thermo Scientific Genesys 10s Ultraviolet-Visible (UV-Vis) spectrophotometer in the wavelength range of 200 to 800 nm.

4.2. Fourier-transform Infrared Spectrometer

All samples were prepared using the KBr pellet technique. Before the quantitative analysis, a fixed mass of GO was accurately weighed and added to a constant mass of KBr (FT-IR grade). The sample pellets were analysed using Perkin Elmer Spectrum 100 Fourier-transform Infrared (FT-IR) spectrometer in the wavenumber region of 4000 to 400 cm^{-1}.

5. Electrochemical Analysis

A three-electrode system composed of a Pt wire electrode (counter; CH instrument), Ag/AgCl electrode (reference; CH instrument) and glassy carbon electrode (working; CH instrument) was constructed for the electrochemical analysis. 2 M H_2SO_4 was used as the electrolyte solution. All electrochemical measurements were performed on Metrohm Autolab PGSTAT M101 potentiostat/galvanostat.

CV analysis is a useful technique commonly used to identify the electrode behaviour and evaluate the specific capacitance of a given sample. The three-electrode system was used to analyse the CV measurements of rGO, 3S-rGO and 5S-rGO in a 2 M H_2SO_4 solution. The formula to calculate the value of specific capacitance from a CV curve is shown below:

$$\text{Specific Capacitance, } F\ g^{-1} = \frac{\int_{v_1}^{v_2} I(V)\, dV}{mk\Delta V} \qquad (1)$$

Where v_1, v_2, m and k represent the value of initial potential (V), final potential (V), the mass of active material (g) and the scan rate (V s^{-1}) respectively. ΔV represents the potential range (V), and the integration of $I(V)dV$ in the potential range gives the area of the CV curve. The CV analysis was performed within the potential window of 0.0 – 1.0 V at different scan rates, ranging from 5 mV s^{-1} to 75 mV s^{-1} for all rGO samples.

RESULTS AND DISCUSSION

1. Chemical Modification of Graphene Oxide using KCl

GO suspension was chemically modified with KCl salt which aggregated GO from the stable suspension.

Figure 1 shows the condition of GO suspension before and after KCl was added and the suspension was left to mix overnight at room temperature. The GO suspension was initially stable in an aqueous solution due to its hydrophilic nature, attributed to the presence of oxygen functional groups on GO. However, the addition of KCl triggered a change in dispersion stability which caused the GO particles to aggregate and sediment.

Hu et al. studied the hydrophilicity of GO and found that it is heavily influenced by parameters such as pH, zeta potential and size of the particle [20]. In this case, it is believed that the instability of GO was influenced by the change in zeta potential for GO dispersion. Typically, GO suspension has a negative zeta potential value due to partial deprotonation of acidic groups [21]. The aggregation of GO particles upon the addition of positive K^+ ions could have been triggered by the reduction in negative charge on GO, causing a shift in zeta potential value which disrupted its dispersion stability.

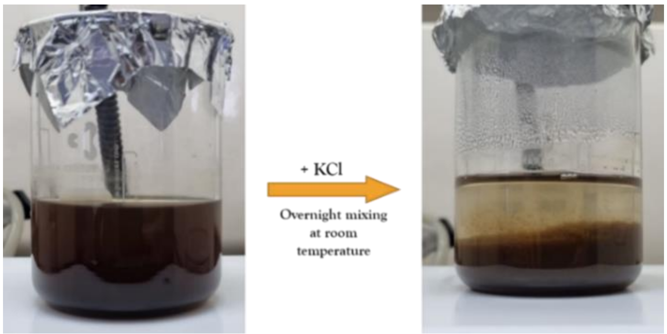

Figure 1. The aggregation of GO after KCl was added.

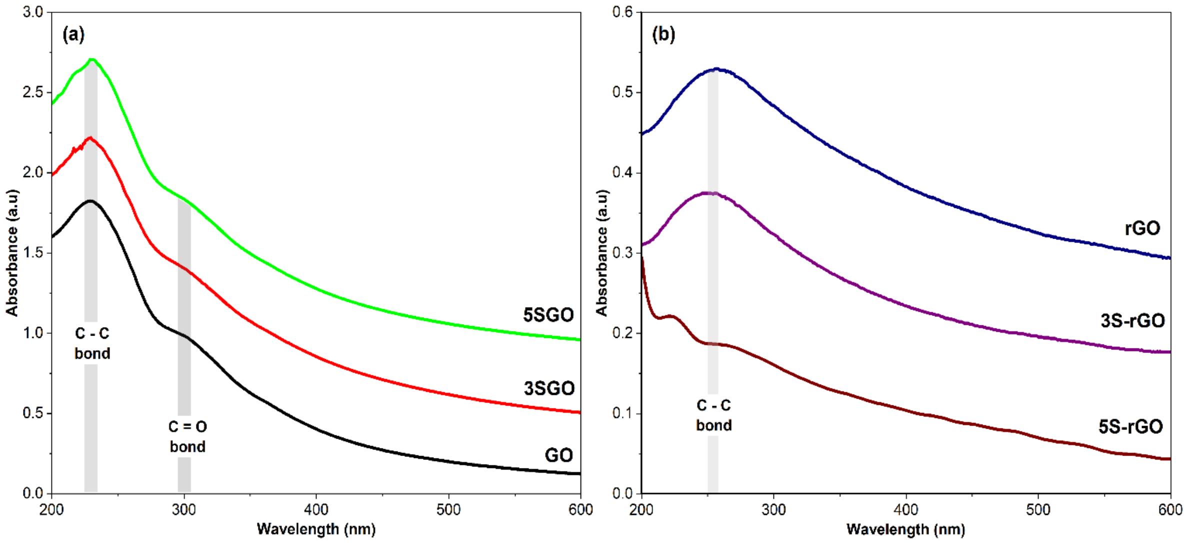

Figure 2. The UV-Vis absorbance spectra of GO (a) and rGO (b) samples.

2. Material Characterisation

2.1. UV-Vis Absorbance Analysis

The UV-Vis absorbance spectra for GO, SGO, rGO and S-rGO samples are shown in Figure 2. GO and SGO samples showed maximum peaks at ~229 nm and moderate shoulders at ~300 nm. The peaks at 229 nm and 300 nm correspond to π-π^* transition due to the formation of aromatic C-C bond and n-π^* transition due to the C=O bond respectively as graphite precursor was oxidised [18]. Absorbance intensity is a useful indicator to estimate the relative abundance of chemical species present in a sample. From Figure 2(a), the absorbance intensities at both wavelengths were significantly more intense for SGO than GO, indicating greater formations of C-C and C=O bonds. This finding can be attributed to further surface oxidation by KCl during the aggregation of GO. 5SGO had the highest intensity at both peak wavelengths, demonstrating that the amount of KCl added can affect the degree of oxidation on the GO surface. In addition, the peak value at ~230 nm can also illustrate that the synthesised GO and SGO samples had a similar hydrodynamic particle size of ~1.5 µm based on work done by Zhang et al. who studied the relationship between UV-Vis peak absorbance and particle size of GO [22].

Next, the peaks redshifted from 229 nm to 257 nm and 251 nm for rGO and 3S-rGO respectively as shown in Figure 2(b), indicating successful restoration of π-conjugation on the graphene layer. No other significant peaks were seen at any other wavelength region which confirms the successful reduction of rGO and 3S-rGO samples using ammonia [18], [23]. Variation in peak wavelengths between rGO and 3S-rGO is believed to have been caused by the difference in the degree of conjugation on the graphene layer. It is reasoned that the degree of reduction on the rGO layer was greater than 3S-rGO which resulted in higher conjugation levels (hence higher wavelength peak value). On the other, 5S-rGO did not show a similar peak shift; instead, the peak at 229 nm was significantly reduced after reduction. It is possible that the positive K^+ ions affected the reduction process by protecting some of the negatively-charged oxygen functionalities through weak interaction, preventing the chemical reaction with ammonia, and affecting the overall degree of reduction [14]. The absorbance intensity for rGO was also higher than 3S-rGO which supports the claim of higher conjugation in the former sample.

2.2. Fourier-Transform Infrared (FT-IR) Analysis

FT-IR analysis was used to detect the presence of functional groups; specifically, the oxygen functionalities on GO and rGO, as well as to support the successful reduction of GO precursors. The interaction between K^+ ions and GO during the chemical modification was evaluated by quantitative analysis of the oxygen functional groups on GO and S-GO samples. The peak area was calculated by integrating the area under the curve for three different peaks; O-H (hydroxyl), C=O (carbonyl/carboxyl) and C-O (epoxy) as shown in Table 1. As the amount of KCl increases, the integrated peak areas for O-H, C=O and C-O decreased with 5SGO having the lowest calculated peak areas for all three oxygen functional groups. The carbonyl/ carboxyl C=O groups had the most drastic change in peak area between GO and SGO samples, nearly halved after GO was modified with KCl. This finding may suggest that K^+ ions have a more significant affinity to the C=O group over other oxygen functionalities. The FT-IR spectra of the GO and rGO samples are illustrated in Figure 3.

When comparing the GO and rGO curves, it can be established that significant amounts of oxygen functional groups had been successfully removed by ammonia solution for all samples except for 5S-rGO. Considerable reduction in transmittance intensity can be observed for O-H (hydroxyl), C=O (carbonyl/carboxyl), C-O (epoxy) and C-H stretching (carbonyl) in rGO and 3S-rGO.

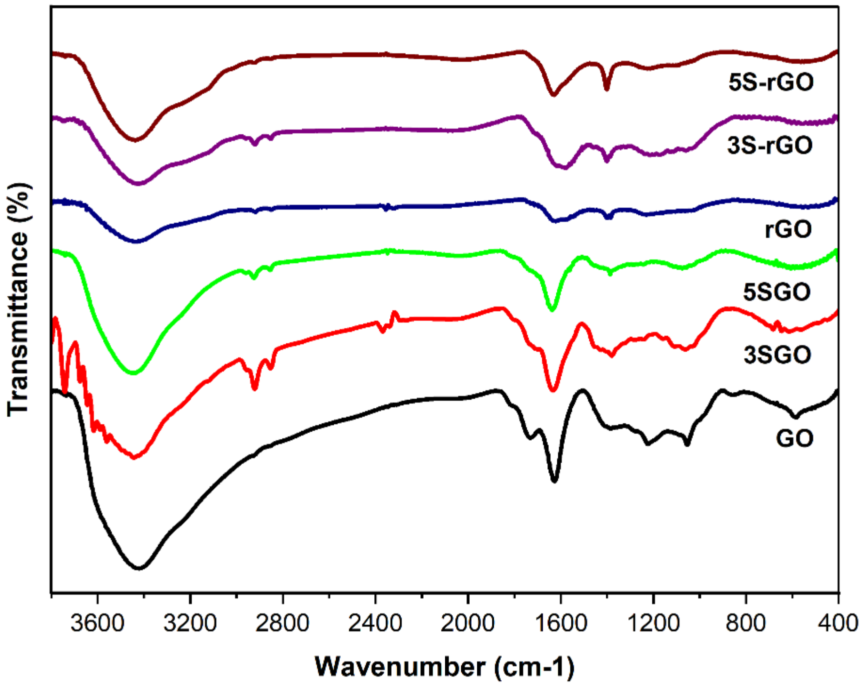

Figure 3. FT-IR spectra of GO and rGO samples.

Table 1. The quantitative peak area of GO, 3SGO and 5SGO.

Functional Groups	Wavenumber Range (cm^{-1})	Calculated Integral Peak Area		
		GO	3SGO	5SGO
O-H (Hydroxyl)	3430 - 3450	3838.42	3364.96	2832.49
C=O (carbonyl/carboxyl)	1700 - 1735	100.06	53.18	49.81
C-O(epoxy)	1070 - 1050	291.62	266.45	203.67

Table 2 summaries the different wavenumber readings with respect to the corresponding functional groups. There are notable differences between the functional groups that existed on rGO and 3S-rGO, namely that the latter had more types of oxygen functionalities present in the reduced form. It can be reasoned that K^+ ions could preserve specific oxygen functional groups such as hydroxyl, carbonyl and epoxy groups through weak intermolecular interaction between positive K^+ ions and negatively-charged oxygen groups [14]. This protection mechanism could have also affected the degree of reduction on SGO samples, forming oxygen-rich S-rGO. This is especially true for 5S-rGO as shown in the spectra which revealed that a significant amount of different oxygen functionalities still existed after the chemical reduction. Hence, increasing the amount of KCl salt added during the modification step can influence the degree of reduction in the products.

Table 2. Summary of FT-IR spectra of rGO, 3S-rGO and 5S-rGO.

Functional Groups	**Wavenumber (cm^{-1})**		
	rGO	**3S-rGO**	**5S-rGO**
O-H (hydroxyl)	3439	3418	3434
C-H stretching (carbonyl)	2847	2853	2853
C-C stretching (aromatic)	1620		1626
O-H bending		1577	
O-H bending (carboxylic)	1398	1403	1403
O-H stretching	1229	1240,1208	1218
C-O stretching (epoxy)		1180,1131,1099,1055	1104

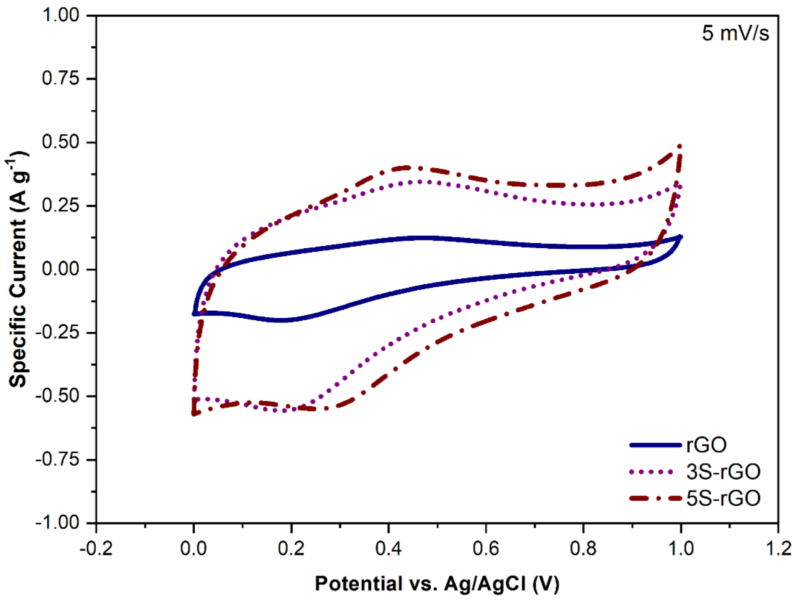

Figure 4. The CV curves for rGO, 3S-rGO and 5S-rGO at 5 mV s^{-1}.

3. Cyclic Voltammetry Analysis

Figure 4 illustrates the CV curves for all samples at 5 mV s^{-1} which behaved similar to a capacitor. The highest calculated specific capacitance (C_{sp}) value was 124.28 F g^{-1} at 5 mV s^{-1} for 5S-rGO, followed by 104.10 F g^{-1} and 35.61 F g^{-1} for 3S-rGO and rGO respectively. The superior capacitive performance of S-rGO samples can be attributed to a hybrid charge storage behaviour that combines the electric double-layer capacitance and pseudo-capacitance due to the rich presence of oxygen functionalities on its surface [8]. This explains the quasi-rectangular- shaped curves for S-rGO due to the reversible faradaic redox reaction that took place on the oxygen functional groups. In contrast, rGO had an almost ideal rectangular shape which signifies a purely electric double-layer capacitance.

Since an acidic electrolyte was used, the main active sites for the redox reactions will take place on the carbonyl and quinone groups as shown in the following equation:

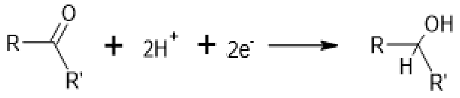

(2)

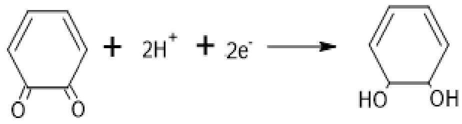

(3)

This mechanism supports the superior capacitive performance of 5S-rGO as it is rich in oxygen functional groups [24], [25].

Figure 5 shows the trend in C_{sp} values for all samples at different scan rates. As the scan rate increases, the calculated C_{sp} value decreases. This trend was caused by the inability of the electrode to cope with the fast electron exchange with electrolyte (due to the high scan rate) which limited effective electrode-electrolyte interaction to the outer electrode surface [26]. Interestingly, the calculated Csp values for S-rGO were more affected at the higher scan rate than rGO. It can be suggested that pseudo-capacitance is significantly affected by the limitation of effective electron exchange at higher scan rates which prevented faradaic redox reaction, contributing to the loss of capacitance [27].

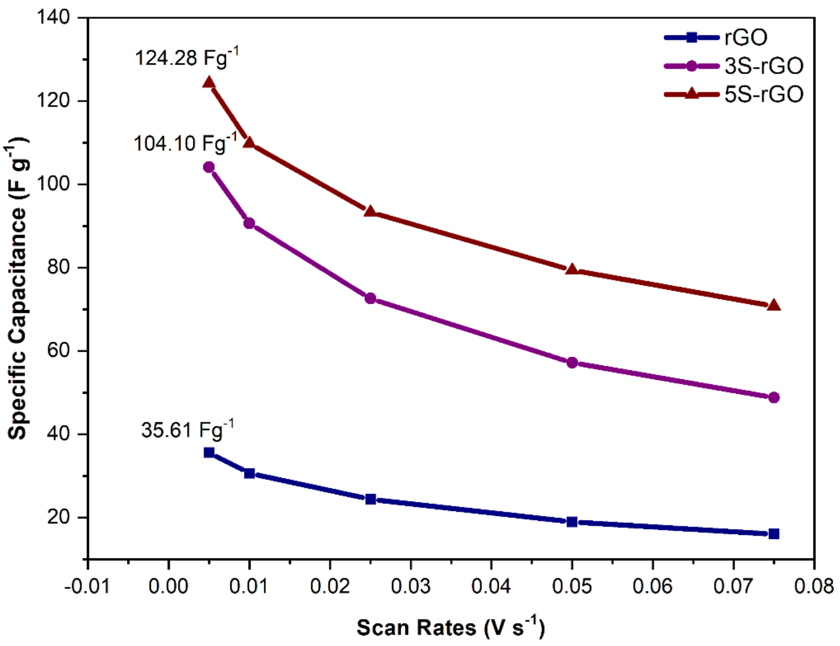

Figure 5. The specific capacitance trend for rGO, 3S-rGO and 5S-rGO.

Table 3. Comparison of the different surface modifications on rGO.

Material	Synthesis Steps	Electrochemical Configuration	Performance	Reference
Thermally-reduced graphene sheets (G-800)	i. Modified Hummers' method. ii. Thermal reduction in argon at 800 °C for 1 hour (G-800). iii. Second oxidation with HNO_3 (OG-800). iv. Metal etching with cobalt acetate (PG).	2-electrode; Ni foam electrode; 5 M KOH electrolyte	At 20 mV s^{-1}; i. G-800: 23 F g^{-1} ii. OG-800: 107 F g^{-1} iii. PG: 27 F g^{-1}	[15]

Hydrothermal N-doped reduced graphene oxide (NrGO)	i. Modified Hummers' method. ii. Sonication of GO: hydrazine suspension iii. Hydrothermal reduction at 180 °C for 12 hours (NrGO)	3-electrode; rGO/PTFE film-coated Pt wire electrode; 6 M KOH electrolyte	At 10 mV s^{-1}; i. rGO: 45 F g^{-1} ii. NrGO: 100 F g^{-1}	[28]
3D oxygen-doped graphene sheets (3D-GN)	i. Commercial GO mixed with NaCl salt. ii. Thermal reduction at 800 °C for 30 mins.	3-electrode; Glassy carbon electrode; 1 M KOH electrolyte	At 1.0 A g^{-1}; i. GN: 52.8 F g^{-1} ii. 3D-GN: 173.5 F g^{-1}	[29]
Chemically modified reduced graphene oxide (S-rGO)	i. Modified Hummers' method. ii. GO aggregation with KCl at room temperature (S-GO). iii. Chemical reduction using hydrazine.	3-electrode; rGO-coated glassy carbon electrode; 2 M H_2SO_4 electrolyte	At 5 mV s^{-1}; i. rGO: 35.6 F g^{-1} ii. 3S-rGO: 104.1 F g^{-1} iii. 5S-rGO: 124.3 F g^{-1}	This work

CONCLUSION

An oxygen-rich S-rGO was successfully synthesised using the environmental-friendly KCl to chemically modify the oxidation level on rGO. It was found that S-rGO had richer oxygen functionalities after the reduction step which observed the incomplete reduction of 5S-rGO whereas 3S-rGO and rGO achieved complete reduction. It was proposed that K$^+$ ions can further oxidise the surface GO and inhibit the removal of oxygen groups during chemical reduction. From the CV analysis. 5S-rGO had the best electrochemical performance with a calculated Csp value of 124.28 F g-1 at 5 mV s^{-1} which is about 3.5 times greater compared to the unmodified rGO. It is believed that this simple modification technique should be considered in large-scale production to manufacture a more environmental-friendly rGO with superior electrode performance for energy storage applications such as supercapacitors or batteries.

ACKNOWLEDGEMENTS

The authors would like to thank the Ministry of Higher Education for the Fundamental Research Grant Scheme (FRGS) (FRGS/1/2020/STG05/UPM/02/3) and Universiti Putra Malaysia for Geran Inisiatif Putra Muda (GP-IPM) (963600) for providing the financial support and facilities for this research.

REFERENCES

1. Feynman, R. P. (1960) There's Plenty of Room at the Bottom. *Engineering and Science,* **23(5)**, 22−36.
2. Taniguchi, N. (1974) On the Basic concept of Nanotechnology. *Proc. Int. Conf. Production Engineering, Tokyo,* **Part II**, 18−23.
3. Madurani, K. A., Suprapto, S., Machrita, N. I., Bahar, S. L., Illiya, W. and Kurniawan, F. (2020) Progress in Graphene Synthesis and its Applications: History, Challenge and the Future Outlook for Research and Industry. *ECS Journal of Solid State Science and Technology*, **9**, 1−12.
4. Bayda, S., Adeel, M., Tuccinardi, T., Cordani, M. and Rizzolio, F. (2020) The History of Nanoscience and Nanotechnology- From Chemical-Physical Applications to Nanomedicine. *Molecules,* **25(112)**, 1−15.
5. Razaq, A., Bibi, F., Zheng, X., Papadakis, R., Jafri, S. H. M. and Li, H. (2022) Review on Graphene-, Graphene Oxide-, Reduced Graphene Oxide-Based Flexible Composites: From Fabrication to Applications. *Materials*, **15**, 1−17.
6. Pomerantseva, E., Bonaccorso, F., Feng, X., Cui, Y. and Gogotsi, Y. (2019) Energy storage: The future enabled by nanomaterials. *Science*, **366**, 1−14.
7. Yu, W., Sisi, L., Haiyan, Y. and Jie, L. (2020) Progress in the functional modification of graphene/graphene oxide: A review. *RSC Advances*, **10**, 15328−15345.
8. Chen, Y., Zhang, Z., Huang, Z. and Zhang, H. (2017) Effects of oxygen-containing functional groups on the supercapacitor performance of

incompletely reduced graphene oxides. *International Journal of Hydrogen Energy*, **42(10)**, 7186–7194.

9. Li, Y., Parrondo, J., Sankarasubramanian, S. and Ramani, V. (2019) Impact of Surface Carbonyl- and Hydroxyl-Group Concentrations on Electrode Kinetics in an All-Vanadium Redox Flow Battery. *Journal of Physical Chemistry C*, **123(11)**, 6370–6378.

10. Greese, T., Loichet Torres, P. A., Menga, D., Dotzauer, P., Wiener, M. and Reichenauer, G. (2021) Impact of Plasma and Thermal Treatment on the Long-term Performance of Vanadium Redox Flow Electrodes – Significance of Surface Structure vs Oxygen Functionalities. *Journal of The Electrochemical Society*, **168**, 1−12.

11. Joshi, Y., Umasankaran, A., Klaassen, C., AlAmer, M. and Joo, Y. L. (2022) Critical roles of reduced graphene oxide in the electrochemical performance of silicon/reduced graphene oxide hybrids for high rate capable lithium-ion battery anodes. *Electrochimica Acta*, **404**, 1-11.

12. Morimoto, N., Kubo, T. and Nishina, Y. (2016) Tailoring the oxygen content of graphite and reduced graphene oxide for specific applications. *Scientific Reports*, **6**, 1−8.

13. Li, R., Yang, Y., Wu, D., Li, K., Qin, Y., Tao, Y. and Kong, Y. (2019) Covalent functionalization of reduced graphene oxide aerogels with polyaniline for high performance supercapacitors. *Chemical Communications*, **55(12)**, 1738–1741.

14. Rajagopalan, B. and Chung, J. S. (2014) Reduced chemically modified graphene oxide for supercapacitor electrode. *Nanoscale Research Letters*, **9**, 1−10.

15. Cao, H., Peng, X., Zhao, M., Liu, P., Xu, B. and Guo, J. (2018) Oxygen functional groups improve the energy storage performances of graphene electrochemical supercapacitors. *RSC Advances*, **8(6)**, 2858–2865.

16. Chen, R., Yu, S., Sun, R. Yang, W. and Zhao, Y. (2012) KCl-assisted, chemically reduced graphene oxide for high-performance supercapacitor electrodes. *Journal of Solid State Electrochem*istry, **16**, 3635–3641.

17. Esencan Turkaslan, B. and Filiz Aydin, M. (2020) Optimizing parameters of graphene derivatives synthesis by modified improved Hummers. *Mathematical Methods in the Applied Sciences*, 1−8.

18. Albarqouni, Y. M. Y., Lee, S. P., Ali, G. A. M., Ethiraj, A. S., Algarni, H. and Chong, K. F. (2021) Facile synthesis of reduced graphene oxide aerogel in soft drink as supercapacitor electrode. *Journal of Nanostructure in Chemistry*, **12**, 417–427.

19. Pham, V. H., Hur, S. H., Kim, E. J., Kim, B. S. and Chung, J. S. (2013) Highly efficient reduction of graphene oxide using ammonia borane. *Chemical Communications*, **49(59)**, 6665–6667.

20. Hu, X., Yu, Y., Hou, W., Zhou, J. and Song, L. (2013) Effects of particle size and pH value on the hydrophilicity of graphene oxide. *Applied Surface Science*, **273**, 118–121.

21. Guimarães, N. R., Nguyen, H. N., Filho, S. S. F. and Rodrigues, D. F. (2020) Removal of graphene oxide from water and wastewater using coagulation–flocculation. *Desalination and Water Treatment*, **173**, 49–56.

22. Zhang, T., Zhu, G. Y., Yu, C. H., Xie, Y., Xia, M. Y., Lu, B. Y., Fei, X. and Peng, Q. (2019) The UV absorption of graphene oxide is size-dependent: possible calibration pitfalls. *Microchimica Acta*, **186**, 1−7.

23. Al-Gaashani, R., Najjar, A., Zakaria, Y., Mansour, S. and Atieh, M. A. (2019) XPS and structural studies of high quality graphene oxide and reduced graphene oxide prepared by different chemical oxidation methods. *Ceramics International*, **45**, 14439–14448.

24. Alireza Hashemi, S., Mojtaba Mousavi, S., Reza Naderi, H., Bahrani, S., Arjmand, M., Hagfeldt, A., Chiang, W. H. and Ramakrishna, S. (2021) Reinforced polypyrrole with 2D graphene flakes decorated with interconnected nickel-tungsten metal oxide complex toward superiorly stable supercapacitor. *Chemical Engineering Journal*, **418**, 1−13.

25. He, Y. Zhang, Y., Li, X., Lv, Z., Wang, X., Liu, Z. and Huang, X. (2018) Capacitive mechanism of oxygen functional groups on carbon surface in supercapacitors. *Electrochimica Acta*, **282**, 618–625.

26. Askari, M. B., Salarizadeh, P., Seifi, M., Rozati, S. M. and Beheshti-Marnani, A. (2020) Binary mixed molybdenum cobalt sulfide nanosheets decorated on rGO as a high-performance supercapacitor electrode. *Nanotechnology*, **31(27)**, 1−21.

27. Fleischmann, S., Mitchell, J. B., Wang, R., Zhan, C., Jiang, D. E., Presser, V. and Augustyn, V. (2020) Pseudocapacitance: From Fundamental Understanding to High Power Energy Storage Materials. *Chemical Reviews*, **120(14)**, 6738–6782.

28. Wang, B., Likodimos, V., Fielding, A. J. and Dryfe, R. A. W. (2020) In situ Electron paramagnetic resonance spectroelectrochemical study of graphene-based supercapacitors: Comparison between chemically reduced graphene oxide and nitrogen-doped reduced graphene oxide. *Carbon*, **160**, 236–246.

29. Li, Z., Li, B., Du, L., Wang, W., Liao, X., Yu, H., Yu, C., Wang, H. and Li, Q. (2021) Three-dimensional oxygen-doped porous graphene: Sodium chloride-template preparation, structural characterization and supercapacitor performances. *Chinese Journal of Chemical Engineering*, **40**, 304–314.